Reac Kinet Mech Cat (2018) 124:247–264
https://doi.org/10.1007/s11144-017-1333-5

Study of the performance of amino-functionalized ordered mesoporous carbon in the transesterification of soybean oil

Amir Hosein Savameri[1,2] · Ali Izadbakhsh[1] · Bahman Zarenezhad[2]

Received: 5 November 2017 / Accepted: 10 December 2017 / Published online: 19 December 2017

Abstract In this study, the synthesis of the amino-functionalized mesoporous carbon resulted from organic–inorganic self-assembly reaction of triblock copolymer P123, sucrose and silica was carried out. The mesoporous carbons with desirable textural properties such as BET surface area of 956 m^2/g, average pore diameter of 4.7 nm and pore volume of 1.07 cm^3/g were obtained. Their surface was modified and functionalized with amine groups. Also, small angle powder X-ray diffraction (XRD) confirmed the hexagonal order of porous structure and Fourier transform infrared (FT-IR) analysis of catalyst indicated presence of amine functional groups onto the surface. FESEM and TEM imaging for the purpose of morphological and structural order analysis have been carried out. The performance of the prepared catalysts was evaluated in the production of biodiesel through transesterification of soybean oil with methanol. Gas chromatography (GC) analysis of biodiesel samples demonstrated that at the temperature of 64 °C, methanol to oil molar ratio of 24:1 and 2 wt% of catalyst loading (based on oil used), about 91% of triglycerides were converted to methyl esters (biodiesel) after 6 h.

Keywords Catalyst · Biodiesel · Amine · Transesterification · Mesoporous · Carbons

Electronic supplementary material The online version of this article (https://doi.org/10.1007/s11144-017-1333-5) contains supplementary material, which is available to authorized users.

✉ Ali Izadbakhsh
izadbakhsh@pgu.ac.ir

Bahman Zarenezhad
bzarenezhad@semnan.ac.ir

[1] Faculty of Petroleum, Gas and Petrochemical Engineering, Persian Gulf University, Bushehr, Iran

[2] Faculty of Chemical, Petroleum and Gas Engineering, Semnan University, Semnan, Iran

Introduction

Biofuel as a renewable source of energy is receiving increasing attention due to environmental concerns involved with the using of fossil fuel resources and their limited capacity to meet the near future world energy demand. Biodiesel can be obtained from animal and vegetable oils. These sources contain high amounts of triglyceride fats, which can be converted to fatty acid esters by transesterification with alcohols. Methanol as a viable industrial alcohol is generally used in transesterification reaction to converts triglycerides to fatty acid methyl esters (FAME) or biodiesel. As a renewable fuel, biodiesel can be produced under standard specifications to be used with or without slight modification in diesel engine. The oxygen content of biodiesel reduces hydrocarbon particulate spread by its combustion. Biodiesel currently is used in some countries as a blend fuel; however, this technology still needs research studies to cope some difficulties.

The transesterification reaction is carried out with acid, base and enzyme catalysts [1, 2]. Homogenous acid/base catalyst is difficult to be separated and their impurities lead to corrosion problems and special metal alloys are needed for process equipment, vessels and piping. The required washing process to separate catalyst and non-converted alcohol produces large amount of waste water polluting the living environment [3–6]. They are in general much less tolerant to water and FFAs in the feedstock. The free fatty acid content found in the vegetable oils with high acid value; especially waste cooking oils, proceeds the saponification reaction with homogenous base catalysts such as potassium hydroxide. Saponification lowers the yield of FAMEs and raises difficulties in the downstream operation due to the formation of emulsions. The fatty acids are pre-esterified with mineral acids followed by several purification steps before transesterification reaction. Therefore, the crude biodiesel fuel obtained by homogenous acid or base catalysts needs to pass through methanol separation, neutralization, wet washing, and drying stages to fulfil biodiesel specifications determined in European or American relevant standards such as EN14214:2012 and/or ASTM D6751 [2, 7].

The immiscible glycerol phase accumulating during the course of the reaction, solubilizes the homogeneous base catalyst and, therefore, withdraws it from the reaction medium and decreases the final yield of FAMEs. Glycerol purification is harder with homogenous transesterification as about 75% purity glycerol can be produced versus 99% in the heterogeneous process [8].

At present, the industrial production of biodiesel is carried out using homogeneous alkaline catalysts such as potassium hydroxide and sodium hydroxide due to easy access and low cost. However, in recent years, studies on the development of heterogeneous acidic or alkaline catalysts have increased in order to overcome the above limitations [1].

Acid heterogeneous catalysts with sulfonic acid groups on different matrixes, such as mesoporous and hierarchic materials [9], zeolites [10], disordered nanoporous carbons [11], and supermicroporous polymers [12–14] have been developed. Alkaline earth metal oxides such as calcium [15] and magnesium oxides [3], tin oxide [16], transition metal oxide, hydrotalcites, and micro and mesoporous

silicates and aluminates impregnated by alkaline agents are the most important heterogeneous basic catalysts [17].

Usage of many metals and metal oxides in the esterification and transesterification processes to produce biodiesel has disadvantages such as high costs, possibility of gas and moisture poisoning of catalysts and detrimental impacts on environment [18, 19]. Hence, the development of supported catalysts having non-metallic alkaline functionalities such as organic amine groups seems to be necessary [20, 21].

Silicates and aluminates are widely used as catalyst supports in biodiesel production through esterification and transesterification processes. Recently, carbon also has gained a desirable position in this area as an optimal and effective catalyst support [22]. It benefits from various porous structures (in spite of the same chemical compositions), remarkable resistance to acidic and alkaline environment, easy access, effective recovery, low density and various ways of production (from cheap raw materials such as wood, coconut shell, coal, etc.), activation and carbonization. For instance, because of desirable pore geometry and volume, activated carbons are used in a broad applications including gas separation and storage, water treatment, catalysis and electrochemistry [23, 24].

The carbons of ordered porous structure have been studied as an amorphous kind of carbonaceous material with controllable structure and pore system, which are synthesized by soft and/or hard casting pathways with relatively high specific surface areas, pore sizes and pore volumes that has made them excellent [24] choices in applications like catalysis and adsorption [17, 24–30].

Besides nanocasting processes with hard templates, which are so much complicated, time consuming and also not possible on an industrial scale, self-assembly methods have been investigated in order to synthesize mesoporous carbons directly using organic templates as structure-directing agents and simultaneously as carbon precursors [31].

This study aimed to synthesize mesoporous carbons with controllable structural properties, using organic–inorganic self-assembly of P123 surfactant, sucrose and silica; and carbonization of this composite at high temperatures. Then, the modification and functionalization of mesoporous carbonaceous supports by organic amine groups and finally, evaluation of performance of prepared catalysts in transesterification of soybean oil (SBO) with methanol, were carried out and the relevant results would be presented and discussed.

Experimental

Chemicals

Pluronic triblock copolymer P123 (99% purity) as surfactant and organic template and n-BuLi (1.6 M solution in hexane) for amination reactions were purchased from Sigma. Tetraethylorthosilicate (TEOS) (98% purity) as silicon source, hydrochloric acid 37%, sulfuric acid, ethanol, sucrose, dried diethyl ether and dried methanol (max 0.003% H_2O) was provided by Merck. 2-Diethylamino ethyl bromide

hydrobromide was obtained from TCI. Soybean oil (OLITALIA soybean oil, SBO) was purchased and used as a triglyceride source. The chemicals were used without further purifications.

Catalyst preparation

Synthesis of carbonaceous support

In order to synthesize the carbon supports, the method used by Ting et al. [31] was followed. For this purpose, chemical materials were mixed in quantities that the final composition of synthesis mixture gives the molar ratios of P123:HCl:H_2O:H_2SO_4: Sucrose: TEOS equal to 1:649:6357:40:7.2:48.3. In a typical synthesis, 1.46 g of P123 as a surface active agent and carbon source was dissolved in a mixture of 36 g of HCl (2 M solution) and 2 g demineralized water at the ambient temperature. Afterwards, the required amount of sucrose as carbon precursor material with 1 g sulfuric acid was added to the solution and stirred for 30 min at the ambient temperature. Then, 2.55 g TEOS as structure direct agent for final carbon material added dropwise and the solution was stirred at the temperature of 50 °C for 24 h. The solution was aged for 24 h at 100 °C in a Teflon autoclave and after that the resulting mixture was dried at 100 °C for 6 h followed by drying at 160 °C for another 6 h. The obtained dark brown colored sediments, then, were carbonized at 900 °C for 12 h under argon flow in order to achieve complete carbonization. To remove the silica template, the obtained black composite was washed in a 2 M NaOH solution with 50:50 water–ethanol solvent at 65 °C for 24 h. Finally, carbonaceous deposits were filtered and washed with plenty of water and ethanol to the neutralization point and dried in atmospheric oven. The obtained carbon material was labeled as OMC.

Amine-functionalization of carbon surface

The procedure used by Villa et al. [32] was utilized for amine modification and functionalization of the carbon supports. 0.5 g of the synthesized carbonaceous supports was dispersed in 100 mL of dried diethyl ether and then excess amount of n-BuLi was added at the ambient temperature under argon flow. After stirring for 5 h, three different amounts of 2-(diethyl amino) ethyl bromide hydrobromide (3, 30 and 50 mmol) were added in the stoichiometric ratio (1:1) with n-BuLi and the suspension was stirred at 35 °C for 90 min. Subsequently, deposits were filtered, rinsed with plenty of methanol and stirred in 100 mL methanol overnight for further lithium removal. Finally, the resulting deposits were filtered, washed with distilled water and methanol, dried at 70 °C overnight and labeled as A/OMC#n, in which n is either 1, 2 or 3 that indicates the lowest, medium and highest amount of amine groups, respectively. The amine molecule binds to the OMC surface via C–C linkage formed between carbon in ethyl bromide branch of amine (E_2NEBr) and surface carbon in OMC attached to Lithium atom (C-Li).

Characterizations

Small angle powder X-ray diffraction (XRD) data were collected using a Philips PW1730 device and Cu K_α ($\lambda = 1.540598$ Å) radiation (40 kV, 30 mA). Nitrogen adsorption–desorption isotherms were obtained at 77 K through a Micromeritics ASAP 2020 surface analyzer with samples degassed under vacuum at 75 °C for 5 h before measurements. The specific surface areas of samples were calculated using BET (Brunauer–Emmett–Teller) method in the relative pressure range of $p/p_0 = 0.05$–0.3. The pore volume and average pore diameter of samples were determined by desorption branch of BJH (Barrett–Joyner–Halenda). FTIR spectra were recorded on a BRAIC WQF-510 FTIR spectrometer using the KBr pellet technique with a wave number range of 400–4000 cm^{-1}. The morphological study of the obtained samples were carried out by means of field emission scanning electron microscopy (FESEM) imaging using a TESCAN MIRA3 set (15 kV). TEM images were prepared on a Philips CM10 at an acceleration voltage of 100 kV. The composition analyses of produced FAME samples were carried out using Agilent technologies 7890A GC set with HP-5 capillary column.

Transesterification

The activity of catalysts was evaluated in the transesterification of soybean oil with methanol. Using a 100 mL three-neck balloon with a water condenser, the transesterification experiments were carried out at the temperature of 64 °C, methanol to oil molar ratio of 24:1 and catalyst (A/OMC#n) concentration of 2 wt% (based on oil weight used) under argon flow. It is noteworthy that before the beginning of reactions, catalysts were oven-dried at 70 °C for 1 h and then cooled in a desiccator. In addition, oil was preheated to the desired reaction temperature and a pre-contact between methanol and catalysts was performed. Product samples were collected every 2 h. In every sample analysis, a sample of 1.0 mL of the reacting mixture was withdrawn periodically followed by centrifugation of samples filled in the vials of 1.5 mL at the rotation speed of 10,000 rpm for 10 min. Without any further heat treatment, after the separation of the catalyst-free products to two phases, the samples of microliter volume of the yellow-color FAME phase were injected to the GC inlet.

The components of methyl ester phase and its composition were determined by gas chromatography. An Agilent 7890 A gas chromatograph equipped with a FID detector and HP-5 capillary column (the length of 30 m, the column internal diameter of 0.32 mm and film thickness of 0.25 μm) with the helium flow as the carrier gas was used for the analysis of biodiesel samples.

In each GC analysis of biodiesel samples, the same optimized analysis method was used as reported elsewhere [16]. The splitted (100:1) injection mode was carried out at the inlet temperature of 280 °C. The oven temperature was kept at 135 °C for 10 min. After that, the oven temperature increased to 170 °C with the temperature ramp of 10 °C/min and remained at 170 °C for 15 min. In the last heating step of the used GC analysis method, the oven temperature increased to 250 °C with the temperature ramp of 25 °C/min, remaining for 2 min at the final

temperature. The FID detector signals were collected at the temperature of 300 °C with the hydrogen flow of 30 mL/min and the air flow of 300 mL/min.

MIX-37 (C_5–C_{25}) from Sigma-Aldrich was used as methyl ester standard to determine FAMEs elution time of the obtained biodiesel samples, given in Table 1, with the above mentioned analysis GC method and the individual response factors obtained via calibration experiments.

The exact weight of methyl esters was obtained from the peak area of each component in the obtained chromatogram after modification with the response factors. The reported FAME yields of transesterification reactions were calculated from the ratio of the weight of the relevant FAME products to the weight of the same quantity of injection of a basis sample of FAMEs. The basis sample of FAMEs was obtained from the complete conversion of the used feedstock oil to FAMEs by a homogenous catalyst, potassium hydroxide, under the conditions of the experiment with the highest obtained FAMEs at each relevant study. The yield of FAMEs, as reported in the following, were calculated from the below formula:

$$\begin{aligned}\text{Yield of FAMEs} &= \left(W_{\text{FAMEs}/W\text{CH}_3\text{OH}}\right)/\left(W_{\text{FAMEs}}/W_{\text{CH}_3\text{OH}}\right)_{\text{Basis Sample}} \\ &= \sum(A_i * f_i)/\sum(A_i * f_i)_{\text{Basis}} * \left(W_{\text{CH}_3\text{OH, Basis}}/W_{\text{CH}_3\text{OH}}\right) \times 100\end{aligned}$$

Here W_i is calculated or measured weight of i, i.e. FAMEs and methanol, A_i is peak area of methyl ester i in chromatogram GC analysis of and f_i is area to weight conversion factors of each component *i* in the FAMEs.

Results and discussion

Catalyst characterizations

The small-angle powder XRD patterns of OMC support and catalyst samples (A/OMC#n) are presented in Fig. 1. As can be seen, the OMC pattern has shown an intense diffraction peak at $2\theta = 1.06$ and two weak diffraction peaks at $2\theta = 1.54$ and 1.72, which can be indicative of the low-index miller planes (100), (110) and (200). This kind of XRD pattern is representative to an ordered material with 2D-hexagonal mesoporous structure with *p6mm* symmetry. Amino-grafted OMC samples demonstrated the same first diffraction reflection with the peaks at the same $2\theta = 1.06$ as for OMC in the low-angle region, indicating the preservation of the

Table 1 Retention time of FAMEs in the methyl esters obtained by transesterification in this work

Component	$C_{17}H_{34}O_2$ (C16:0)	$C_{17}H_{32}O_2$ (C16:1)	$C_{19}H_{38}O_2$ (C18:0)	$C_{19}H_{36}O_2$ (C18:1n9c)	$C_{19}H_{34}O_2$ (C18:2n6c)
Name	Methyl palmitate	Methyl palmitoleate	Methyl stearate	Cis-9-oleic methyl ester	Methyl lineolate
Retention time, min	19.51	18.889	21.913	21.751	21.644

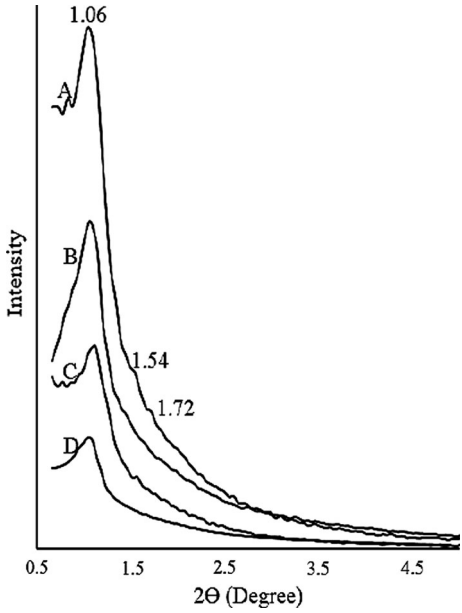

Fig. 1 Small angle powder XRD patterns for samples OMC (*A*), A/OMC#1 (*B*), A/OMC#2 (*C*) and A/OMC#3 (*D*)

hexagonal mesostructure of OMC supports with reduced order due to the reduction of intensity of the first peak and the loss of the other two relevant peaks. No significant shift of the first diffraction reflection with the amination intensity was observed, indicating that the d-spacing of crystallographic planes of carbon cylindrical pores structure remains unchanged. In other words, the required synthesis steps for the amination of OMC have no effect on the distance of parallel silica nanorods. In addition, with the binding of amine functional groups to the carbonaceous material, the intensity of the first reflection was declined and the last two weak reflections were disappeared. This can be explained with the partial reduction in the order quality of mesoporous structure [33].

The specific surface area, and the average pores diameter and volume of samples were calculated form data of nitrogen adsorption–desorption isotherms using the BET model and BJH model. Nitrogen adsorption–desorption isotherms of all samples are shown in Fig. 2. These isotherms are of type IV, which represents the mesoporous characteristic of the samples OMC and A/OMC#n. In addition, the hysteresis loops in isotherms are combinations of type H1 and H4, which indicate the presence of long cylindrical mesopores located in the matrix of smaller ones [34]. A large portion of the pore structure with the pore diameter of 4.72 nm in the prepared carbonaceous material (OMC) is originated from the dissolution of SBA-15 silica walls in the initial composite [31]. The minor portion may be attributed to the pores of larger diameter, resulting from carbon dissolution of material in the basic solution.

The results of surface analysis including BET surface areas and pore diameters and volumes are presented in Table 2. The results clearly indicate the reduction of surface areas and pore sizes of carbonaceous support (OMC) after functionalization

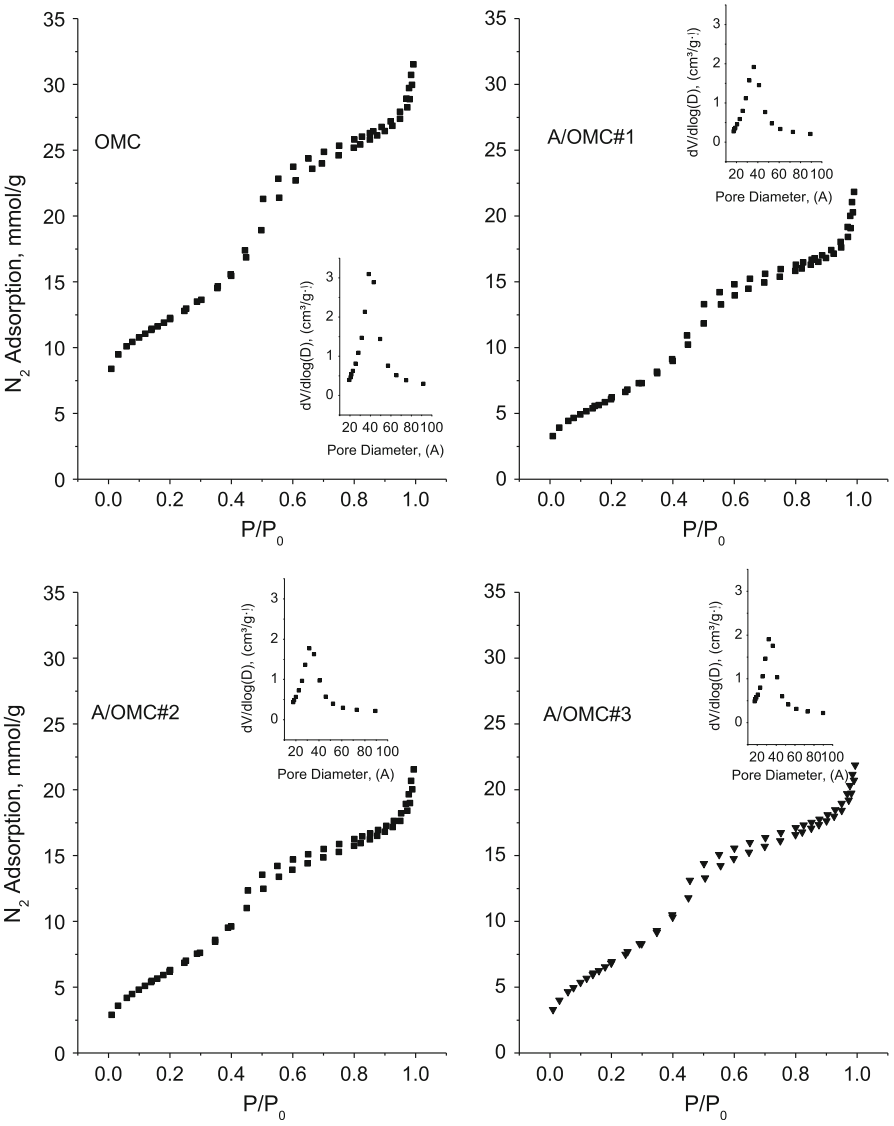

Fig. 2 Nitrogen adsorption–desorption isotherms of samples OMC, A/OMC#1, A/OMC#2, and A/OMC#3 with the pores size distribution as the inset figures

as a result of the addition of alkaline organic amine agents to the porous carbonaceous material. This treatment reduced the surface area of OMC to about 50% of the initial value. The size of pores exhibited a reduction from 4.72 to less than 4.44 nm and pores volume decreased from 1.07 to about 0.78 cm^3/g. The volume of pores remains nearly content, *ca*. 0.8 cm^3/g, with increase of amination intensity of OMC. Therefore, the major reduction of surface area and pore volume can be attributed to the pore aperture plugging by tri-alkyl amine and the subsequent

Table 2 Textural properties of samples OMC and A/OMC#n obtained from Nitrogen adsorption–desorption isotherms

Sample	BET surface area (m^2/g)	Pore diameter (nm)	Pore volume (cm^3/g)
OMC	956	4.72	1.07
A/OMC#1	505	4.44	0.78
A/OMC#2	533	4.09	0.77
A/OMC#3	584	3.99	0.79

decreased rate of pore diffusion. The increased amount of amine in the synthesis mixture, resulted in the moderate increase of the surface areas of A/OMC#n and slight reduction of the pore sizes of the aminated samples. The increase of amination intensity may increase the number of larger pore formed through intensified carbon dissolution. Compared to these larger pores, the smaller pores originated from silica dissolution faces a stronger pore blockage by bulky tri-ethyl amine. The former effect enhances the surface area, whereas the latter results in the reduction of surface area due to both of the smaller pore size and the stronger pore blockage. The results of surface analysis showed that the effect of carbon dissolution had the dominant increasing influence on the surface area with no variation of the pores volume. With the increase of amination intensity, the intensity of the first XRD reflection signal in Fig. 1 is reduced which may support formation of new pores with different d-spacing after amine treatment of samples.

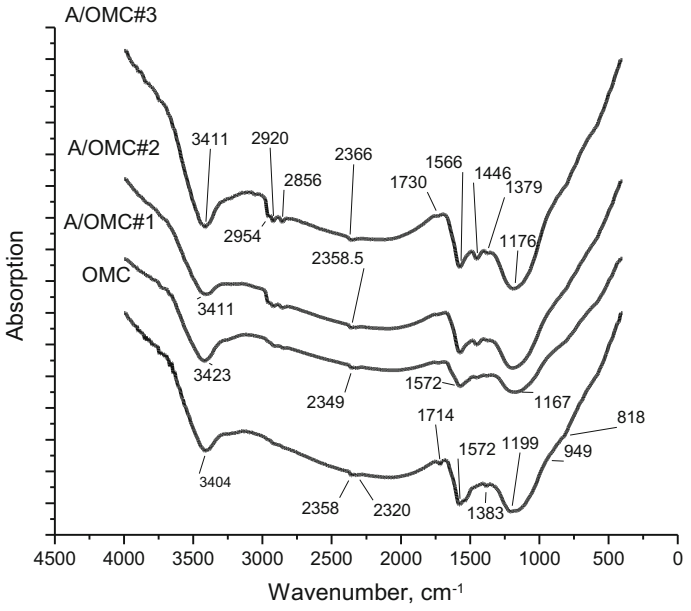

Fig. 3 FTIR spectra of samples OMC, A/OMC#1, A/OMC#2 and A/OMC#3

FTIR spectra of samples OMC and A/OMC#n are represented in Fig. 3. As can be seen, some typical bands of a carbon material (OMC) in wavenumbers such as 818, 949 and 1199 cm^{-1} are observed which are attributed to out of plane bending of aromatic C–H bonds, out of plane bending of alkyne C–H bonds, and vibration of C–O–C bonds, respectively.

The bands at the wavenumbers of 1383 and 1446 cm^{-1} were assigned to $–CH_3$ bending vibrations, which are continuously intensified with the amine content in the FTIR spectrum of the amine-functionalized OMC samples. The relevant vibrations of aromatic C–C bond, C=O (carbonyl) bond, and alkyne C≡C (stretching) appeared at the wavenumbers of 1556, 1730, and 2360.

Moreover, the bands at the wavenumbers of (2856, 2954) and 2920 cm^{-1} were assigned to the (symmetric and asymmetric) stretching vibrations of $-CH_3$ bonds and $–CH_2–$ [35] attached to the nitrogen atom of amine functional group, respectively. No significant variation of the intensity of the band at the 3411 cm^{-1} was observed in the spectra of amine-functionalized samples as an evidence for stretching vibration of N–H (primary amine). Therefore, the band at 3411 cm^{-1} was assigned to the stretching vibration of surface OH bond. This and the presence of relevant bands of bending and stretching vibrations of $–CH_3$ and $–CH_2–$ have confirmed the major part of amine functional group anchored to the surface of mesostructured carbon is the tertiary type [35].

The FESEM micrographs of samples OMC and A/OMC#n for the purpose of morphological analysis are given as supplementary information. According to the micrographs, the morphology of the rope-like mesoporous carbon fibers bundle, which is same as that usually observed for the ordered mesoporous silica SBA-15, preserves after the functionalization process with the different amounts of organic amine groups. These observations are in agreement with the results of other characterization analyses including XRD and BET. In addition, the similar morphologies between the OMC supports and SBA-15 mesoporous silica proved the successful structure transformation from silica to that of OMCs. In addition, the aggregation and binding of more numbers of carbonaceous strings together with the increase of amine loading in A/OMC#1 to A/OMC#2 and A/OMC#3 is observed in FESEM images.

Carbon fiber bundles were enlarged with amination intensity. The dimensions of carbon fiber bundles were increased from *ca*. 2×10 μm^2 in OMC sample to the sizes of about 6×20 μm^2 in sample A/OMC#3. It indicates the basicity of solution in the amination step promotes the agglomeration of carbon rods together, leading to the less dispersed and longer carbon fiber bundles.

TEM images of mesoporous carbonaceous support sample (OMC) are given in Fig. 4. The parallel array of carbon nano-rods is clearly observed in the side view image. Therefore, TEM images represent another evidence of successful transferring the pore structure of parent silica SBA-15 to the resultant mesoporous carbon. From the TEM images, carbon nano-rods with the diameters of 2–4 nm can be recognized.

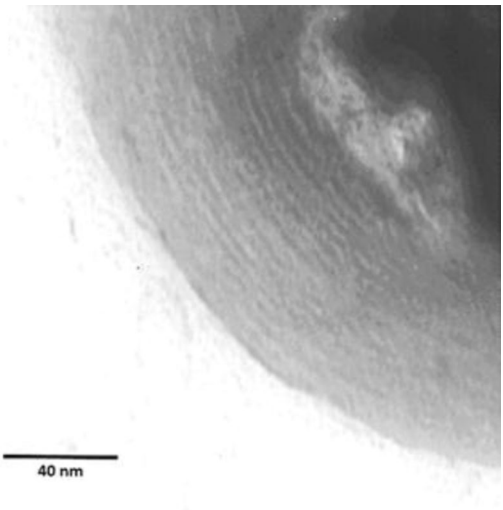

Fig. 4 TEM image of carbonaceous support sample OMC

Performance in the transesterification reaction

Fig. 5 shows the effect of increasing the amount of amine functional groups onto the surface of OMCs on the catalytic activity of prepared A/OMC#n catalysts in the transesterification of Soybean oil with methanol. With an increase of the active sites density of the amine group on the OMC supports, more alkaline sites are available to convert the glyceride molecules. Therefore, as can be seen in Fig. 5, by increasing the amine loading on OMCs, conversion of triglycerides to fatty acid methyl esters (FAME) proceed to the higher conversions at the same reaction time. A/OMC#1 sample produced no considerable FAMEs with time (FAMEs yield of

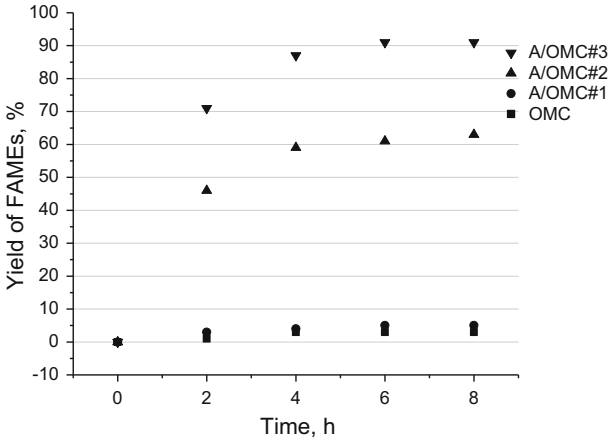

Fig. 5 Catalytic performance of OMC, A/OMC#1, A/OMC#2 and A/OMC#3 catalysts in terms of conversion of triglycerides to FAMEs at the reaction temperature of 64 °C, methanol to oil molar ratio of 24:1, and catalyst concentration of 2 wt%

less than 5%), whereas A/OMC#2 and A/OMC#3 catalyst samples converted the soybean oil to FAMEs by 61% and 9% after 6 h.

The faster kinetics of the transesterification reaction with the A/OMC#3 catalyst under reaction conditions compared with that of the A/OMC#2 catalyst can be deduced from the steeper initial slope of the corresponding yield curve in Fig. 5. After 2 h of reaction, the A/OMC#3 catalyst converted the soybean oil by *ca*.70% (80% of its equilibrium yield) well above that of the A/OMC#2 catalyst.

In addition, the transesterification reaction was carried out using the OMC support as a catalyst to investigate its activity. Using OMC as a catalyst led to the negligible conversion of feedstock oil, *ca*. about 3%, to FAMEs. It indicated the low activity of the bare support and substantial impact of amino-functional organic groups on the catalytic activity of the prepared samples. The minor observed conversion of transesterification via non-aminated OMC sample can be attributed to the surface OH groups with the assigned wavenumber in the FTIR spectrum.

Table 3 illustrates the basic site densities of different catalysts and their transesterification activities in the reaction runs at the conditions of 64 °C, methanol to oil molar ratio of 24:1, catalyst loading of 2 wt% and 8 h of reaction time. The basic site density was measured by acid-base titration using HCl as titrant and a 10^{-3} M KCl solution for dispersion of catalysts. A linear relation of the transesterification reaction conversion with the catalyst basic density was observed from data in Table 3, proposing a single-site catalytic mechanism for the reaction.

Fig. 6 illustrates the yield of FAMEs with time at the different methanol to oil molar ratio in the transesterification of soybean oil with A/OMC#3 catalyst. FAMEs yield increased significantly as methanol to oil ratio increased from 12 to 24 at the same time of reaction using A/OMC#3 catalyst. With the increase of methanol to oil molar ratio from 12 to 18 in the reaction mixture with A/OMC#3 catalyst, the yield of triglyceride conversion to FAMEs increases from 38 to 59% after 8 h. A further increase of the methanol to oil molar ratio to 24, transesterification reaction moves forwards, leading to the FAMEs yield of 89% at the reaction time of 8 h. Comparing to homogenous basic catalyst, it was observed that the large methanol to oil ratio is required for catalyst of highest amine content to obtain an acceptable rate of transesterification reaction. This may be a result of the steric hindrance imposed by methyl or ethyl group(s) of amine centers on the reactant molecule preventing them from an easy access to the surface nitrogen atoms.

Table 3 Catalytic activities and basic sites densities of catalysts with different content of amine functional groups

Catalyst	Basic sites density (mmol/g)	Catalyst activity (FAME yield %)[a]
A/OMC#1	0.07	5
A/OMC#2	0.68	63
A/OMC#3	0.89	91

[a]Reaction conditions: reaction temperature of 64 °C, methanol to oil molar ratio of 24:1, catalyst loading of 2 wt%, and time of reaction of 8 h

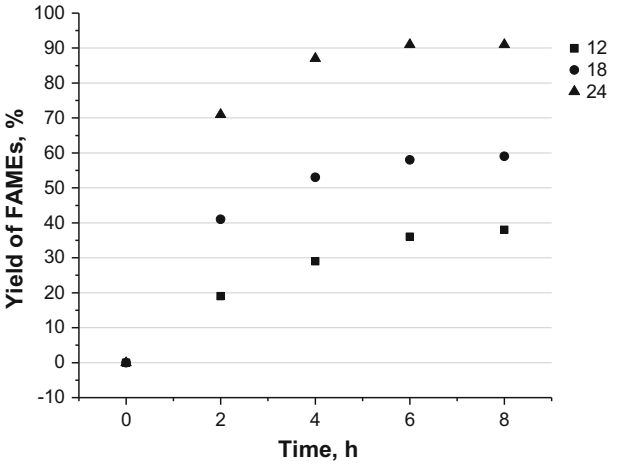

Fig. 6 Yield of FAMEs versus time at the different methanol to oil molar ratio (12, 18, 24) in the transesterification conversion with A/OMC#3 catalyst at the reaction temperature of 64 °C, catalyst loading of 2 wt%

The yield of the transesterification reaction versus time at the different temperatures, given in Fig. 7, confirmed the strong effect of temperature in the range of study. Therefore, temperature was an effective factor on the increasing yield of reaction. With increasing the temperature from 50 to 64 °C, a strong promotion of FAME yield from 29% to 89% was obtained with A/OMC#3 catalyst at the reaction time of 8 h. However, further increase of temperature to 80 °C did not enhance the yield of FAME significantly. Increasing the reaction temperature, in addition to enhancement of reaction rate, could result in the reduced viscosity of

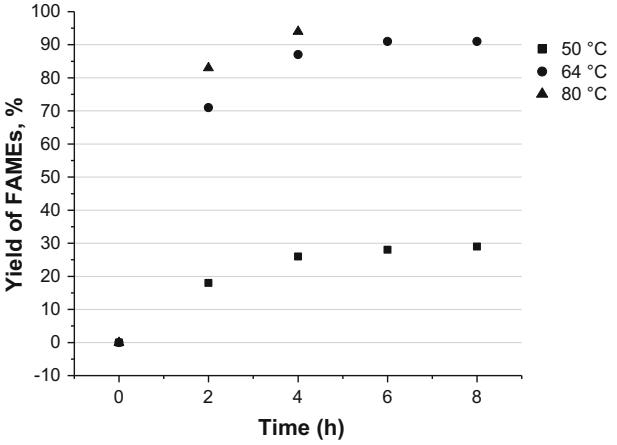

Fig. 7 Yield of FAMES versus time at the different Temperatures (50, 64, 80 °C) in the transesterification conversion to FAMEs with A/OMC#3 catalyst at the conditions of methanol to oil ratio of 24, catalyst loading of 2 wt%

mixture, intensified rate of mass transfer and enhanced phase mixing [16]. The formation of methanol bubbles in the temperature higher than 65 °C considerably trades off the positive effect of temperature on the yield of FAMEs. The formation of bubbles and subsequent reduced methanol concentration in the reaction mixture resulted in the less increase of reaction yield with the temperature above 65 °C.

Optimum reaction conditions of methyl ester yield produced via transesterification of soybean oil using basic heterogeneous catalysts such as Mg–Al hydrotalcite, Li/MgO, CaO supported on mesoporous silica or alumina were given in Table 4. The best reported performance includes FAMEs yield of approximately 100% with sodium silicate under conditions of 7.5:1 alcohol/oil molar ratio, 3 wt% catalyst amount, 1 h reaction time and 60 °C reaction temperature. The prepared aminated OMC sample needs much higher excess proportion of methanol:Oil (24:1) with catalyst amount = 2 wt% to give rise to the maximum FAMEs yield of 94 wt% at 80 °C after 4 h.

Calcium oxide, CaO, is the most widely used as a solid basic catalyst for transesterification as it presents many advantages such as long catalyst life, high activity and requires only moderate reaction conditions. Beside, CaO has attracted

Table 4 Soybean transesterification with solid catalysts

Catalyst	Optimum reaction conditions	Biodiesel FAME yield (%)	References
Li/MgO	T = 60 °C, t = 2 h Methanol/oil = 12:1 Catalyst amount = 9 wt%	93.9	[36]
KI/Mg–Al mixed-metaloxides	T = 60 °C, t = 8 h Methanol/oil = 16:1 Catalyst amount = 5 wt%	> 90	[37]
Mg–Al hydrotalcite	T = 230 °C, t = 1 h Methanol/oil = 13:1 Catalyst amount = 5 wt%	90	[38]
CaO/mesoporoussilica	T = 60 °C, t = 8 h Methanol/oil = 16:1 Catalyst amount = 5 wt%	95.2	[39]
Sodium silicate	T = 60 °C, t = 1 h Methanol/oil = 7.5:1 Catalyst amount = 3 wt%	≈ 100	[40]
CaO/Alumina	T = 65 °C, t = 5 h Methanol/oil = 12:1 Catalyst amount = 6 wt%	98.6	[41]
Phosphazenium hydroxide/SiO_2	T = 75 °C, t = 12 h Methanol/oil = 60:1 Catalyst amount ≈ 3.8 wt%	≈ 100	[42]

much attention due to the fact that there are several natural calcium sources from wastes, such as egg shells or mollusk shells. The reported performance of CaO supported on mesoporous silica is comparable to catalyst A/OMC#3, though at lower methanol:oil ratio (16:1), but at the expense of the higher catalyst dosage and the longer reaction time for the former catalyst [39]. The performance of CaO supported on alumina is slightly better than catalyst A/OMC#3 at much less methanol:oil ratio (12:1) but with three-fold catalyst usage [41]. It is expected that a further increase of amine content of OMC should enhance its catalytic performance for transesterification of soybean oil at less methanol:oil ratio.

The physical properties of the feedstock soybean oil and the biodiesel produced by A/OM:C#3 catalyst were given in Table 5. The acid content of soybean oil reduced by 50% in the obtained biodiesel. The kinematic viscosity of biodiesel (7.9 mm^2/s) requires more reduction to meet the relevant specification of EN14214 standard. If the high viscosity of the obtained FAME is originated from unreacted triglycerides remained in the FAME phase, the adjustment of amine content to a larger quantity could be a possible solution to the problem. The density of biodiesel sample is acceptable based on the range determined in the EN14214 standard.

Catalyst reusability and stability tests

One of the most important and essential parameters of heterogeneous catalysts is their reusability in successive catalytic cycles. As mentioned earlier, this parameter is one of the advantages over the homogeneous catalysts because of environmental and economical point of view. For this purpose, the A/OMC#3 catalyst was separated from the reaction mixture after each catalytic run by vacuum filtration and washed several times with n-hexane and methanol in order to remove the adsorbed nonpolar and polar impurities. Finally, the washed catalysts were dried at 80 °C for 6 h and reserved in a desiccator.

Fig. 8 demonstrates the catalyst stability and reusability after four catalytic cycles. It can be observed that after the first to the third catalytic cycles, the activity of the catalyst is reduced slightly. This activity reduction can be due to the negligible leaching of active amine sites into the reaction medium and/or possible chemisorption of methyl esters products on the amine sites present on the external

Table 5 Physical properties of feedstock oil and biodiesel produced by A/OMC#3 catalyst

Sample	Acid content, mg KOH/g	Kinematic viscosity at 40 °C, mm^2/s	Density, g/cm^3 at 15 °C
Soybean oil	0.34	28.6	0.92
Biodiesel sample	0.18	7.9	0.89
Biodiesel ASTM (D6751) standard	Max 0.5	1.9–6	–
Biodiesel EN (EN14214) standard	Max 0.5	3.5–5	0.86–0.90

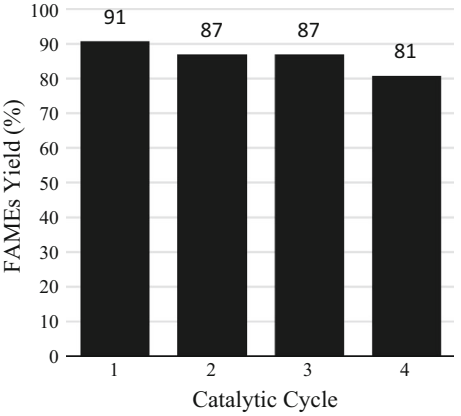

Fig. 8 Reusability tests for the A/OMC#3 catalyst at the reaction temperature of 64 °C, methanol to oil molar ratio of 24:1, catalyst loading of 2 wt%, and reaction time of 6 h

surface or pores of carbonaceous supports via amide bond formation ($RCON(Et)_2$-surface). The evaporation of amine functional groups of catalyst material by sequential drying at the temperature of 80 °C is another possible reason. Since organic amine groups are anchored to the supports by covalent bonds, their leaching possibility is much less than that of chemisorptive blockage of active sites.

Conclusions

Amine functionalized ordered mesoporous carbons (OMC) were synthesized using organic–inorganic self-assembly of triblock copolymer P123, silica and sucrose followed by a previously examined amination recipe. Desirable textural and surface properties including pore size of 4–4.4 nm with the hexagonal order of pore network and the surface area of 500–580 m^2/g were confirmed for these carbonaceous materials, making them good choices as catalyst supports in transesterification of soybean oil with methanol. Alkaline organic amine functional groups, grafted onto the surface of prepared OMCs as catalyst support, catalyzed the transesterification reaction catalysis effectively. About 91% conversion of triglycerides to FAME was obtained using catalyst A/OMC#3 with the highest amine content at the reaction temperature of 64 °C, methanol to oil molar ratio of 24:1, catalyst concentration of 2 wt% and reaction time of 8 h. The rather high molar ratio of methanol to oil was required to obtain the large FAMEs yields of *ca*. 90%. Additionally, admissible stability was observed for the above-mentioned catalyst. The decrease in the yield of FAMEs was measured as large as 4%, from 91 to 87%, after three successive cycles of catalytic conversion.

Acknowledgements The financial support of Vice-Presidency for Science and Technology, Presidency of the Islamic Republic of Iran is gratefully acknowledged. We acknowledge Shakhe Zeytoon Lian Inspection for its generous support.

References

1. Lam MK, Lee KT, Mohamed AR (2010) Homogeneous, heterogeneous and enzymatic catalysis for transesterification of high free fatty acid oil (waste cooking oil) to biodiesel: a review. Biotechnology advances, vol 28. Elsevier Inc. https://doi.org/10.1016/j.biotechadv.2010.03.002
2. Guldhe A, Singh B, Mutanda T, Permaul K, Bux F (2015) Advances in synthesis of biodiesel via enzyme catalysis: novel and sustainable approaches. Renew Sustain Energy Rev 41:1447–1464
3. Manríquez-Ramírez M, Gómez R, Hernández-Cortez JG, Zúñiga-Moreno A, Reza-San Germán CM, Flores-Valle SO (2013) Advances in the transesterification of triglycerides to biodiesel using MgO–NaOH, MgO–KOH and MgO–CeO2 as solid basic catalysts. Catal Today 212:23–30. https://doi.org/10.1016/j.cattod.2012.11.005
4. Zhang L, Guo W, Liu D, Yao J, Ji L, Xu N, Min E (2008) Low boiling point organic amine-catalyzed transesterification for biodiesel production. Energy Fuels 22:1353–1357. https://doi.org/10.1021/ef700636u
5. Crabbe E, Nolasco-Hipolito C, Kobayashi G, Sonomoto K, Ishizaki A (2001) Biodiesel production from crude palm oil and evaluation of butanol extraction and fuel properties. Process Biochem 37:65–71. https://doi.org/10.1016/S0032-9592(01)00178-9
6. Abreu FR, Lima DG, Hamú EH, Wolf C, Suarez PAZ (2004) Utilization of metal complexes as catalysts in the transesterification of Brazilian vegetable oils with different alcohols. J Mol Catal A: Chem 209:29–33. https://doi.org/10.1016/j.molcata.2003.08.003
7. Chen SY, Mochizuki T, Abe Y, Toba M, Yoshimura Y, Somwongsa P, Lao-ubol S (2016) Carbonaceous Ti-incorporated SBA-15 with enhanced activity and durability for high-quality biodiesel production: synthesis and utilization of the P123 template as carbon source. Appl Catal B 181:800–809. https://doi.org/10.1016/j.apcatb.2015.08.053
8. Sivasamy A, Cheah KY, Fornasiero P, Kemausuor F, Zinoviev S, Miertus S (2009) Catalytic applications in the production of biodiesel from vegetable oils. Chemsuschem 2(4):278–300
9. Lee AF, Wilson K (2015) Recent developments in heterogeneous catalysis for the sustainable production of biodiesel. Catal Today 242:3–18
10. Helwani Z, Othman MR, Aziz N, Kim J, Fernando WJN (2009) Solid heterogeneous catalysts for transesterification of triglycerides with methanol: a review. Appl Catal A 363:1–10
11. Tamborini LH, Casco ME, Militello MP, Silvestre-Albero J, Barbero CA, Acevedo DF (2016) Sulfonated porous carbon catalysts for biodiesel production: clear effect of the carbon particle size on the catalyst synthesis and properties. Fuel Process Technol 149:209–217
12. Kundu SK, Bhaumik A (2015) Pyrene-based porous organic polymers as efficient catalytic support for the synthesis of biodiesels at room temperature. ACS Sustain Chem Eng 3:1715–1723
13. Bhunia S, Banerjee B, Bhaumik A (2015) A new hypercrosslinked supermicroporous polymer, with scope for sulfonation, and its catalytic potential for the efficient synthesis of biodiesel at room temperature. Chem Commun 51:5020–5023
14. Farzaneh F, Moghzi F, Rashtizadeh E (2016) Zn (II) coordination polymer as a bifunctional catalyst for biodiesel production from soybean oil. Reac Kinet Mech Cat 118(2):509–521
15. Kouzu M, Kasuno T, Tajika M, Sugimoto Y, Yamanaka S, Hidaka J (2008) Calcium oxide as a solid base catalyst for transesterification of soybean oil and its application to biodiesel production. Fuel 87:2798–2806. https://doi.org/10.1016/j.fuel.2007.10.019
16. Goudarzi F, Izadbakhsh A (2017) Evaluation of K/SnO_2 performance as a solid catalyst in the transesterification of a mixed plant oil. React Kinet Mech Catal 121:539–553
17. Zabeti M, Wan Daud WMA, Aroua MK (2009) Activity of solid catalysts for biodiesel production: a review. Fuel Process Technol 90:770–777. https://doi.org/10.1016/j.fuproc.2009.03.010
18. Yu D, Nagelli E, Du F, Dai L (2010) Metal-free carbon nanomaterials become more active than metal catalysts and last longer. J Phys Chem Lett 1:2165–2173
19. Jin X, Balasubramanian VV, Selvan ST, Sawant DP, Chari MA, GeQ Lu, Vinu A (2009) Highly ordered mesoporous carbon nitride nanoparticles with high nitrogen content: a metal-free basic catalyst. Angew Chem 121:8024–8027
20. Yuan C, Chen W, Yan L (2012) Amino-grafted graphene as a stable and metal-free solid basic catalyst. J Mater Chem 22:7456–7460
21. Su DS, Zhang J, Frank B, Thomas A, Wang X, Paraknowitsch J, Schlögl R (2010) Metal-free heterogeneous catalysis for sustainable chemistry. Chemsuschem 3:169–180

22. Zu Y, Liu G, Wang Z, Shi J, Zhang M, Zhang W, Jia M (2010) CaO supported on porous carbon as highly efficient heterogeneous catalysts for transesterification of triacetin with methanol. Energy Fuels 24:3810–3816. https://doi.org/10.1021/ef100419m
23. Konwar LJ, Boro J, Deka D (2014) Review on latest developments in biodiesel production using carbon-based catalysts. Renew Sustain Energy Rev 29:546–564
24. Yang Y, Chiang K, Burke N (2011) Porous carbon-supported catalysts for energy and environmental applications: a short review. Catal Today 178:197–205
25. Zhang B, Zhou Q, Wang Y, Song N, Ni L (2017) Synthesis of ordered mesoporous carbon using m-Diethynylbenzene as a new precursor. Mater Lett 189:317–320
26. Oschatz M, Thieme S, Borchardt L, Lohe MR, Biemelt T, Brückner J, Althues H, Kaskel S (2013) A new route for the preparation of mesoporous carbon materials with high performance in lithium–sulphur battery cathodes. Chem Commun 49:5832–5834
27. Li J, Liang Y, Dou B, Ma C, Lu R, Hao Z, Xie Q, Luan Z, Li K (2013) Nanocasting synthesis of graphitized ordered mesoporous carbon using Fe-coated SBA-15 template. Mater Chem Phys 138:484–489
28. Han B-H, Zhou W, Sayari A (2003) Direct preparation of nanoporous carbon by nanocasting. J Am Chem Soc 125:3444–3445
29. Lu A-H, Schüth F (2005) Nanocasting pathways to create ordered mesoporous solids. C R Chim 8:609–620
30. Ryoo R, Joo SH, Jun S (1999) Synthesis of highly ordered carbon molecular sieves via template-mediated structural transformation. J Phys Chem B 103:7743–7746
31. Ting C-C, Wu H-Y, Vetrivel S, Saikia D, Pan Y-C, Fey GTK, Kao H-M (2010) A one-pot route to synthesize highly ordered mesoporous carbons and silicas through organic–inorganic self-assembly of triblock copolymer, sucrose and silica. Micropor Mesopor Mater 128:1–11. https://doi.org/10.1016/j.micromeso.2009.07.018
32. Villa A, Tessonnier J-P, Majoulet O, Su DS, Schlögl R (2010) Transesterification of triglycerides using nitrogen-functionalized carbon nanotubes. Chemsuschem 3:241–245. https://doi.org/10.1002/cssc.200900181
33. Ka Shah, Parikh JK, Maheria KC (2014) Biodiesel synthesis from acid oil over large pore sulfonic acid-modified mesostructured SBA-15: process optimization and reaction kinetics. Catal Today 237:29–37. https://doi.org/10.1016/j.cattod.2014.04.028
34. Lu A-H, Zhao D, O'Brien P, Craighead H, Kroto H (2009) Nanocasting. P001–P266. https://doi.org/10.1039/9781847559869
35. Lambert JB, Shurvell HF, Cooks RG (1987) Introduction to organic spectroscopy. Macmillan, New York, pp 174–177. https://doi.org/10.1007/s11746-015-2722-4
36. Wen Z, Yu X, Tu S-T, Yan J, Dahlquist E (2010) Synthesis of biodiesel from vegetable oil with methanol catalyzed by Li-doped magnesium oxide catalysts. Appl Energy 87(3):743–748
37. Tantirungrotechai J, Chotmongkolsap P, Pohmakotr M (2010) Synthesis, characterization, and activity in transesterification of mesoporous Mg–Al mixed-metal oxides. Micropor Mesopor Mater 128(1):41–47
38. Silva CCC, Ribeiro NF, Souza MM, Aranda DA (2010) Biodiesel production from soybean oil and methanol using hydrotalcites as catalyst. Fuel Process Technol 91(2):205–210
39. Samart C, Chaiya C, Reubroycharoen P (2010) Biodiesel production by methanolysis of soybean oil using calcium supported on mesoporous silica catalyst. Energy Convers Manage 51(7):1428–1431
40. Guo F, Peng Z-G, Dai J-Y, Xiu Z-L (2010) Calcined sodium silicate as solid base catalyst for biodiesel production. Fuel Process Technol 91(3):322–328
41. Zabeti M, Daud WMAW, Aroua MK (2010) Biodiesel production using alumina-supported calcium oxide: an optimization study. Fuel Process Technol 91(2):243–248
42. Kim MJ, Kim M-Y, Kwon OZ, Seo G (2011) Transesterification of vegetable oils over a phosphazenium hydroxide catalyst incorporated onto silica. Fuel Process Technol 92(1):126–131